Journal of Organometallic Chemistry, 206 (1981) 265—277
Elsevier Sequoia S.A., Lausanne — Printed in The Netherlands

A REINVESTIGATION OF *o*-PHENYLENEMERCURIALS

IV *. ADDUCTS OF PERFLUOROTRIBENZO[*b*,*e*,*h*][1,4,7]TRIMERCURONIN AND THE CRYSTAL AND MOLECULAR STRUCTURE OF ITS 1 : 1 4-PHENYLPYRIDINE SOLVATE

MATTHEW C. BALL, DAVID S. BROWN, ALAN G. MASSEY * and DENYS A. WICKENS

Department of Chemistry, University of Technology, Loughborough, LE11 3TU (Great Britain)

(Received August 20th, 1980)

Summary

Perfluorotribenzo[*b*,*e*,*h*][1,4,7]trimercuronin forms adducts of 1 : 1, 1 : 2 and 1 : 3 stoicheiometry with a variety of polar organic molecules. The structure of the 1 : 1 adduct with 4-phenylpyridine was solved by X-ray methods to an *R* factor of 7.4% for 3528 observed reflections.

We have recently shown that *o*-phenylenemercury is trimeric in both its crystal forms [1,2]. The perfluoro analogue $(C_6F_4Hg)_n$ is considered to be trimeric [3] but it was found to differ from $(C_6H_4Hg)_3$ by crystallizing out of *N*,*N*-dimethylformamide with several molecules of solvent of crystallization. A series of exploratory experiments showed that similar solvates were formed between perfluorotribenzo[*b*,*e*,*h*][1,4,7]trimercuronin and a variety of polar organic molecules. As organomercurials do not normally form complexes we decided to investigate these solvates further in an attempt to deduce the nature of the interaction between the ligands and $(C_6F_4Hg)_3$.

Experimental

Perfluorotribenzo[*b*,*e*,*h*][1,4,7]trimercuronin was prepared by a modification of Sartori's decarboxylation method [3] as described previously [4]. In the case of adducts formed with liquid solvents, preparation was effected by

---

* For part III see ref. 4.

simple recrystallisation, whereas adducts of solid "ligands" were obtained by mixing ethanolic solutions of the two compounds in the correct stoicheiometric ratios. The thermogravimetric analytical data were obtained using a Stanton-Redcroft TG750 thermobalance, with a flowing nitrogen atmosphere maintained above all the samples. The data obtained were interpreted as described in the literature [5,6]. Microanalyses were carried out by the University of Manchester Microanalytical Laboratory. Infra-red spectra were recorded on a Perkin Elmer 457 spectrometer using liquid paraffin or hexachlorobutadiene mulls between caesium iodide discs. Raman spectra were recorded on a Cary 81 spectrometer between 100 cm^{-1} and 4000 cm^{-1}; far infra-red spectra were recorded between 32 cm^{-1} and 400 cm^{-1} on a Perkin Elmer 180 spectrometer using liquid paraffin mulls and polyethylene optics. ^{19}F NMR spectra were recorded on a Perkin Elmer R32 spectrometer using C_6F_6 at 163.0 ppm as an external standard. UV spectra were obtain from a Unicam SP800 spectrometer.

Single crystals of the 1 : 1 adduct with 4-phenylpyridine were examined using a Stoë automatic 2-circle Weissenberg geometry diffractometer fitted with a graphite monochromator. Crystallographic calculations were performed using the SHELX suite of programs [7], as implemented at the University of Manchester Regional Computer Centre and on the MULTAN 74 package [8] at Loughborough. Thermal elipsoid plots were calculated using the ORTEP package [9]. A crystal (0.077 × 0.170 × 0.56 mm) was mounted about the crystallographic *a* axis for collection of numerical data.

Results

Adducts formed

The following compounds formed adducts:

Amides

DMF, dimethylformamide
DEF, diethylformamide
DMA, dimethylacetamide
DPF, diphenylformamide

Amines

4-phenylpyridine
quinoline
4-picoline
3-picoline
2-picoline
2,6-lutidine
pyridine

Others

DMSO, dimethylsulphoxide
acetone
triphenylphosphine
cyclopentanone
cyclohexanone

Analytical data

Only a few of the adducts formed were stable enough to be analysed. Table 1 gives analytical data for these. Evidence of partial decomposition is obvious for some compounds.

Thermal analysis

Figure 1 shows typical TG and DTA traces for one of the more stable adducts (2 DMF). These were run on freshly prepared compounds and the TG trace shows well-defined plateaux corresponding to 2 DMF, DMF and parent mercurial. The DTA trace, however, indicates that the second weight loss is

TABLE 1

MICRO-ANALYSIS RESULTS (%)

Complex [a]	Analysis. Found (calcd.) (%)			
	C	H	N	F
I	21.1(21.2)	0.2(0.0)	0.0(0.0)	22.2(22.4)
I. DMF	22.5(22.4)	0.6(0.65)	1.3(1.29)	21.0(21.1)
I. 2 DMF	24.2(24.17)	1.1(1.17)	2.1(2.35)	19.4(19.14)
I. 2 DEF	27.2(26.8)	1.8(1.76)	2.2(2.2)	
I. 2 DMA	25.8(25.6)	1.5(1.47)	2.5(2.3)	
I. py	26.0(24.5)	0.5(0.4)	1.4(1.2)	
I. 1(2-pic)	22.4(25.2)	0.5(0.6)	0.9(1.2)	
I. 2(3-pic)	30.1(29.2)	1.3(1.1)	2.7(2.3)	
I. 2(4-pic)	27.5(29.2)	0.9(1.1)	1.9(2.3)	
I. (2,6-lut)	25.8(26.0)	1.0(0.8)	1.5(1.2)	
I. (4-Ph-py)	30.6(28.9)	1.0(0.7)	1.6(1.2)	
I. 2(DMSO)	21.4(21.9)	1.0(1.0)	0.0(0.0)	
I. C_5H_8O	24.4(24.4)	0.7(0.7)	0.0(0.0)	

[a] I = parent mercurial.

probably occurring in two stages. The 2 DMF adduct does not begin to decompose until ~325 K, thus giving ample time for purification and handling. The analytical data in Table 1 confirm the overall stability of the 2 DMF adduct.

Less stable behaviour, as represented by the 3 DMA adduct is shown in Figure 2, which indicates that decompositon begins as soon as the temperature exceeds ambient. The weight losses agree reasonably with the suggested stoicheiometry, although there is again DTA evidence for multistage decomposition.

It proved possible to study most of the adducts by TG and this was used (a) to indicate the stoicheiometry of the starting material and the likely decomposition reactions, and (b) to decide on temperatures for isothermal decom-

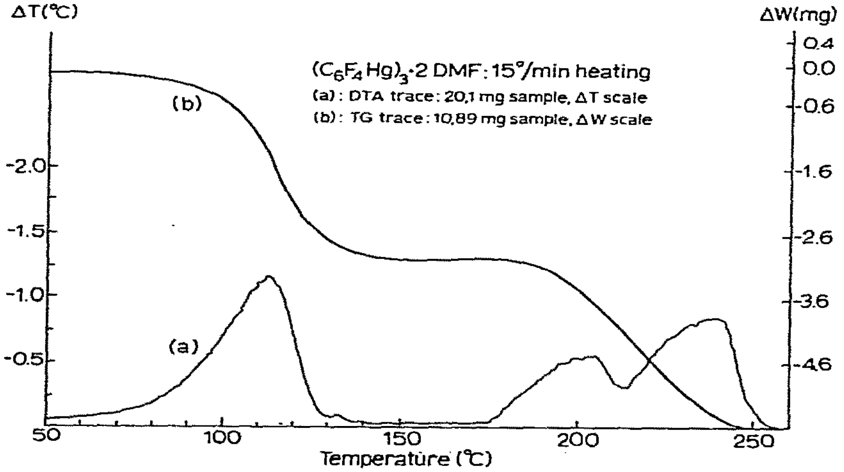

Fig. 1. Thermogravimetric and DTA traces for $(C_6F_4Hg)_3 \cdot 2$ DMF.

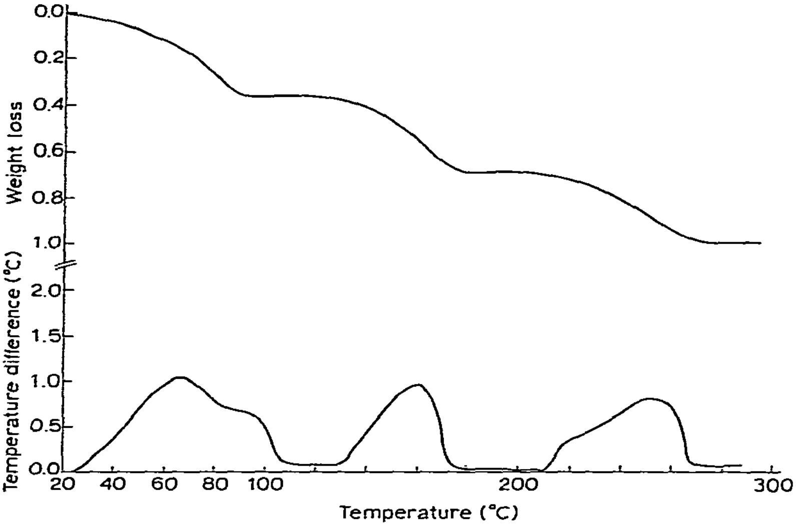

Fig. 2. Thermogravimetric and DTA traces for $(C_6F_4Hg)_3 \cdot 3$ DMA.

position studies. These were generally chosen to be as low as possible, reducing the possibility of overlap of consecutive reactions.

Isothermal decompositions

Table 2 gives the experimental temperatures used and the stoicheiometries obtained for the decompositions studied. The likely reaction mechanisms have been obtained by the method of reduced-time plots, in which the experimental time-proportion decomposed data are fitted to a series of model equations covering possible rate-controlling steps. The steps considered were nucleation of product, growth (phase boundary control) and diffusion control, each having several possible geometric constraints. This allows a "best fit" between experiment and model to be decided on. Table 2 also indicates such "best-fit" mechanisms for the decompositions studied. All of the lower temperature mechanisms indicate phase boundary control of the decompositions; a few become diffusion controlled at higher temperatures as might be expected. Changes in the formal geometry of the various decomposition processes with temperature may not be significant.

The reaction mechanisms having been decided on, the TG traces were then reanalysed by the method of Satava and Skvara to derive Arrhenius parameters which are given in Table 3. Only reactions which yielded unambiguous mechanism data have been included. Included in this table for comparison are results for certain cobalt-pyridine complexes. Attempts to prepare and study a number of other mercury compounds and complexes with pyridine were hampered by high volatility or complicated decomposition patterns.

Infra-red spectroscopy

Early attempts to obtain solution spectra for some of the adducts indicated extensive decomposition; solutions smelled strongly of the ligand, whereas the

TABLE 2

REACTION MECHANISMS FOR THE LOSS OF SOLVENT FROM ADDUCTS OF PERFLUORO-*o*-PHENYLENEMERCURY, I, AND FOR $CoCl_2py_4$ AND HgI_2py_2

Reaction	Temperature(s) (K)	"Best-fit" mechanism(s) [a]
2 DMF.I → 1 DMF.I	340, 350	C.D.
1 DMF.I → I	425	C.D.
	447, 459	C.S.
3 DMA.I → 2 DMA.I	288	C.D.
2 DMA.I → 1 DMA.I	351	C.D.
	377, 379, 382, 392, 410	C.D.
1 DMA.I → I	437	C.D.
	467, 482, 493	C.S.
3 DEF.I → 2 DEF.I	316, 319, 331, 340	C.D.
	312	C.S.
	314	C.D.
2 DEF.I → 1 DEF.I	354, 370, 397	C.D.
	386, 393	C.S.
	404	P.L.
1 DEF.I → I	427	C.S.
	433	C.S.
	440	C.S.
	442	P.L.
	458, 463	P.L.
3 py.I → 1 py.I	311, 320, 325, 332	C.D.
1py. I → I	356	C.D.
	360	C.D.
	375	C.S.
	406	C.S.
3(2-pic).I → 2(2-pic).I	291	C.D.
2(2-pic).I → I	318	C.S.
	325	C.S.
1(4-phenylpyridine).I → I	384, 406	C.S.
2(triphenylphosphine).I → I	421, 434	C.D.
$CoCl_2py_4 \rightarrow CoCl_2py_2$	318, 334, 345, 346	C.D.
$CoCl_2py_2 \rightarrow CoCl_2py$	381, 391, 399, 402, 407, 417	C.D.
$CoCl_2py \rightarrow CoCl_2py_{2/3}$	469	C.S.
	486	P.L.
$CoCl_2py_{2/3} \rightarrow CoCl_2$	521	C.D.
	559	C.S.
$HgI_2py_2 \rightarrow HgI_2$	326	C.D.
	334	C.S.

[a] C.D., Contracting disc equation, $1 - (1 - \alpha)^{1/2} = kt$.
C.S., Contracting sphere equation, $1 - (1 - \alpha)^{1/3} = kt$.
P.L., Parabolic law, $\alpha^2 = kt$.

solids did not, but in addition there was no shift in the carbonyl band frequency with polar solvents. The carbonyl stretching mode was the only solvent band to show slight shifts on adduct formation and some of these shifts are given in Table 4. The absorption attributed [10] to C—N bending, at 653 cm^{-1}, is unaffected in both DMF and DEF adducts (Table 5). Similarly the "umbrella" mode in pyridine at 703 cm^{-1} is unchanged in its 1 : 1 and 1 : 3 adducts despite reports of its sensitivity to complexation [11].

Far infra-red examination was made of the parent mercurial and four of its

TABLE 3

ACTIVATION ENERGIES AND FREQUENCY FACTORS FOR THE LOSS OF SOLVENT FROM ADDUCTS OF PERFLUORO-*o*-PHENYLENEMERCURY, I, AND FOR $Copy_4Cl_2$ [a]

Reaction	Activation energy (kJ mol^{-1})	Frequency factor (sec^{-1})
2 DMF.I → 1 DMF.I	91	1.4×10^{14}
1 DMF.I → I	107	9.7×10^{13}
2 DMA.I → 1 DMA.I	107	1.9×10^{12}
1 DMA.I → I	124	6.7×10^{11}
2 DEF.I → 1 DEF.I	124	6.7×10^{17}
3 py.I → 1 py.I	140	7.2×10^{13}
1 py.I → I	124	9.7×10^{13}
1(4-phenylpyridine).I → I	91	2.1×10^{15}
2(triphenylphosphine).I → I	107	1.9×10^{15}
α-$CoCl_2py_2$ → $CoCl_2py$	91	1.1×10^{10}
$CoCl_2py$ → $CoCl_2py_{2/3}$	140	2.3×10^{14}
$CoCl_2py_{2/3}$ → $CoCl_2$	156	1.3×10^{14}

[a] Results are ±16 kJ mol^{-1}.

adducts (with DMF and py), since proof of coordination-complex formation would have been supplied by absorption in this region which would be absent in the separate spectra. These bands occur at about 120—140 cm^{-1} for mercury-pyridine complexes [11]. As an extra check the 1 : 1 adduct with deuteropyridine was also investigated, as an isotopic shift would provide additional proof of a pyridine-sensitive absorption. No extra bands were visible in any of the 1 : 1 adduct spectra.

The only real change in the mercurial component of the IR spectra is in the splitting of the band at 1098 cm^{-1}; this band is also moved to lower energy. The splitting is probably due to a slight change in molecular geometry expected when extra molecules are co-crystallised. The slight nature of the shift indicates that deviation from D_{3h} point symmetry is small. (See Figure 3).

Raman spectroscopy

Spectra were taken on powder samples of the parent mercurial and DMF and DEF adducts. All of these exhibited severe broad band fluorescence.

TABLE 4

POSITION OF C=O STRETCHING MODE (cm^{-1}) IN ADDUCTS $(C_6F_4Hg)_3.L_n$

L	"Free"	$n = 1$	$n = 2$	$n = 3$
DMF	1670	1645	1660	—
DEF	1675	1630	1643, 1630	1660
DPF	1718; 1706	1650	—	—
DMA	1640	1593	1604	1614
Acetone [a]	1712	1682	—	—
Cyclopentanone [a]	1750; 1740	1780	—	—

[a] Stoicheiometry of adduct not established.

TABLE 5

POSITION OF O=C—N BENDING MODE (cm^{-1}) IN ADDUCTS $(C_6F_4Hg)_3 \cdot L_n$

L	"Free"	$n = 1$	$n = 2$	$n = 3$
DMF	660	665	661	—
DEF	647	645	642	645

X-ray crystallography

Crystal data. $C_{29}H_9F_{12}Hg_3N$, $M = 1201$, Monoclinic, $a = 11.22(1)$, $b = 27.31(2)$, $c = 9.53(1)$ Å, $\beta = 105.2(1)°$, $U = 2818.2$ Å^3, $D_x = 2.83$ Mgm^{-3}, $Z = 4$, $F(000) = 2152$, Cu-K_α radiation, $\lambda = 1.54178$ Å, $\mu = 30.1$ mm^{-1}. Absent reflections, $0k0$ when $k \neq 2n$, $h0l$ when $h + l \neq 2n$, conform uniquely with the space group $P2_1/n$ (No. 14).

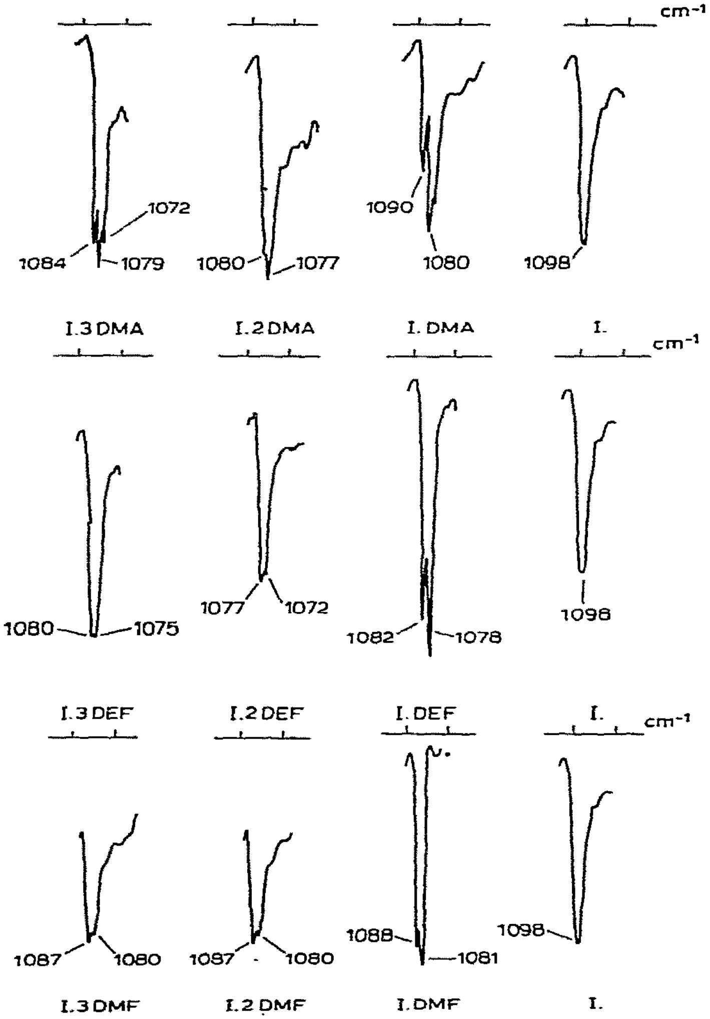

Fig. 3. Infrared spectra in the 1080 cm^{-1} region for various adducts.

TABLE 6

POSITIONAL PARAMETERS ($\times 10^4$) WITH THEIR E.S.D.'S IN PARENTHESES

	x	*y*	*z*
Hg(1)	8212(1)	3359(0)	7389(1)
Hg(2)	4911(1)	3287(0)	6066(1)
Hg(3)	6376(1)	4451(0)	6963(1)
C(1)	3874(26)	3921(10)	5874(28)
C(2)	4433(25)	4388(9)	6316(27)
C(3)	3704(30)	4801(11)	6238(33)
C(4)	2447(31)	4772(11)	5797(33)
C(5)	1904(32)	4337(12)	5422(36)
C(6)	2646(28)	3912(11)	5482(31)
F(3)	4274(16)	5236(6)	6639(18)
F(4)	1788(18)	5179(7)	5811(21)
F(5)	677(20)	4296(7)	5009(22)
F(6)	2021(18)	3489(7)	5112(21)
C(11)	8309(26)	4483(9)	7512(28)
C(12)	9019(28)	4059(10)	7751(31)
C(13)	10 248(29)	4096(11)	8186(32)
C(14)	10 862(31)	4548(11)	8474(33)
C(15)	10 106(28)	4966(10)	8280(31)
C(16)	8893(27)	4920(10)	7895(29)
F(13)	11 017(17)	3704(7)	8326(20)
F(14)	12 056(18)	4592(7)	8919(19)
F(15)	10 664(18)	5405(7)	8608(20)
F(16)	8209(16)	5342(6)	7802(18)
C(21)	6020(27)	2662(10)	6437(29)
C(22)	7286(25)	2689(9)	6977(27)
C(23)	7959(29)	2256(11)	7275(33)
C(24)	7336(30)	1795(11)	7074(32)
C(25)	6160(30)	1778(11)	6540(32)
C(26)	5486(29)	2199(11)	6225(32)
F(23)	9199(16)	2255(6)	7808(18)
F(24)	8077(17)	1390(7)	7397(20)
F(25)	5569(18)	1344(7)	6336(20)
F(26)	4216(16)	2154(6)	5712(18)
C(31)	4347(29)	2835(11)	9333(32)
C(32)	4915(29)	2383(11)	9676(33)
C(33)	4260(32)	1955(12)	9350(36)
N(34)	2971(27)	1969(10)	8766(30)
C(35)	2470(33)	2387(12)	8380(37)
C(36)	3116(29)	2856(11)	8639(32)
C(41)	5120(29)	3317(11)	9736(32)
C(42)	4445(31)	3749(12)	9855(35)
C(43)	5041(35)	4185(13)	10 261(39)
C(44)	6437(34)	4172(13)	10 550(38)
C(45)	6936(35)	3769(13)	10 448(39)
C(46)	6317(28)	3316(11)	9990(31)

The 3528 reflections where $I \geqslant 4\sigma(I)$ were classed as observed, and corrected for Lorentz, polarisation and absorption effects. Inter-layer scale factors were refined (during isotropic structure refinement, then held constant) since some decomposition of the crystal in the beam was apparent. The structure was solved for heavy atoms using direct methods [8], and a difference map obtained after anisotropic refinement of the trial structure with the highest figure of merit revealed all of the non-hydrogen light atoms. Isotropic refinement of these parameters lead R to converge at 7.4%. Final positional parameters are

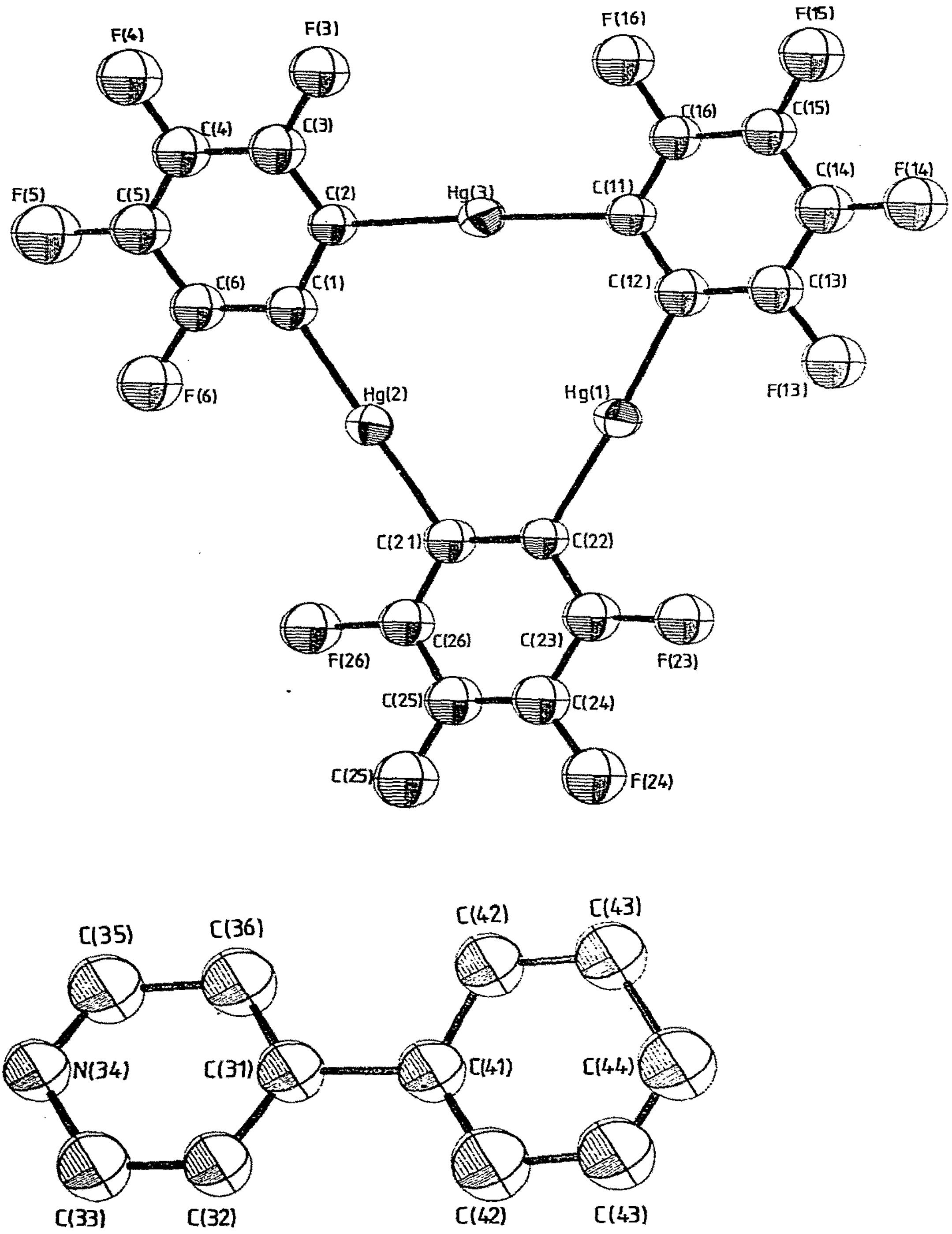

Fig. 4(a) and 4(b). Atom numbering scheme for the $(C_6F_4Hg)_3$ - 4-phenyl pyridine adduct.

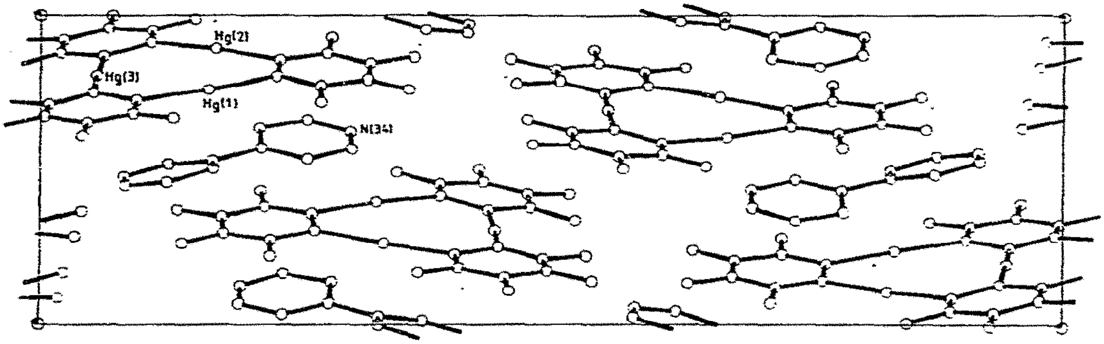

Fig. 5. Unit cell contents for the $(C_6F_4Hg)_3$ · 4-phenyl pyridine adduct.

listed in Table 6 with the atom numbering and molecular structure being shown in Figure 4. The unit cell contents are shown in Figure 5.

Discussion

The adducts of perfluorotribenzo[*b*,*e*,*h*][1,4,7]trimercuronin are interesting because spectroscopic investigation could not unequivocally determine the nature of the bonding. The shifts in carbonyl infra-red absorption in solvents containing this functional group and the splitting of the mercurial band at 1098 cm^{-1} indicate that some interaction is taking place, yet donor-acceptor com-

TABLE 7

BOND LENGTHS (Å) WITH THEIR E.S.D.'S

Hg(1)—C(12)	2.10(3)	Hg(1)—C(22)	2.09(3)
Hg(2)—C(1)	2.07(3)	Hg(2)—C(21)	2.09(3)
Hg(3)—C(2)	2.11(3)	Hg(3)—C(11)	2.10(3)
C(1)—C(2)	1.43(4)	C(1)—C(6)	1.33(4)
C(2)—C(3)	1.38(4)	C(3)—C(4)	1.37(4)
C(4)—C(5)	1.34(4)	C(5)—C(6)	1.42(4)
C(3)—F(3)	1.36(3)	C(4)—F(4)	1.34(3)
C(5)—F(5)	1.33(4)	C(6)—F(6)	1.35(3)
C(11)—C(12)	1.39(4)	C(11)—C(16)	1.37(4)
C(12)—C(13)	1.34(4)	C(13)—C(14)	1.41(4)
C(14)—C(15)	1.41(4)	C(15)—C(16)	1.32(4)
C(13)—F(13)	1.36(3)	C(14)—F(14)	1.30(4)
C(15)—F(15)	1.35(3)	C(16)—F(16)	1.37(3)
C(21)—C(22)	1.38(4)	C(21)—C(26)	1.39(4)
C(22)—C(23)	1.39(4)	C(23)—C(24)	1.43(4)
C(24)—C(25)	1.29(4)	C(25)—C(26)	1.37(4)
C(23)—F(23)	1.35(3)	C(24)—F(24)	1.37(3)
C(25)—F(24)	1.35(3)	C(26)—F(26)	1.39(3)
C(31)—C(32)	1.39(4)	C(31)—C(36)	1.37(4)
C(32)—C(33)	1.37(4)	C(33)—N(34)	1.41(4)
N(34)—C(35)	1.28(4)	C(35)—C(36)	1.46(4)
C(41)—C(42)	1.42(4)	C(42)—C(46)	1.30(4)
C(42)—C(43)	1.37(4)	C(43)—C(44)	1.52(5)
C(44)—C(45)	1.25(5)	C(45)—C(46)	1.43(4)
C(31)—C(41)	1.57(4)		

TABLE 8

BOND ANGLES (°) AND THEIR E.S.D.'S

C(22)—Hg(1)—C(12)	175.9(1.1)	F(14)—C(14)—C(13)	123.7(2.8)
C(1)—Hg(2)—C(21)	175.3(1.0)	F(14)—C(14)—C(15)	120.2(2.8)
C(2)—Hg(3)—C(11)	176.7(1.0)	F(15)—C(15)—C(14)	117.6(2.7)
Hg(1)—C(12)—C(11)	121.7(2.2)	F(15)—C(15)—C(16)	122.1(2.6)
Hg(1)—C(12)—C(13)	119.0(2.2)	F(16)—C(16)—C(15)	117.2(2.5)
Hg(1)—C(22)—C(21)	122.0(1.9)	F(16)—C(16)—C(11)	119.7(2.5)
Hg(1)—C(22)—C(23)	119.3(2.1)	C(26)—C(21)—C(22)	117.8(2.6)
Hg(2)—C(1)—C(2)	121.7(2.0)	C(21)—C(22)—C(23)	118.7(2.5)
Hg(2)—C(1)—C(6)	121.8(2.1)	C(22)—C(23)—C(24)	120.1(2.8)
Hg(2)—C(21)—C(26)	120.2(2.1)	C(23)—C(24)—C(25)	120.2(3.1)
Hg(2)—C(21)—C(22)	122.0(2.0)	C(24)—C(25)—C(26)	120.5(3.1)
Hg(3)—C(2)—C(1)	119.8(1.9)	C(25)—C(26)—C(21)	122.7(2.9)
Hg(3)—C(2)—C(3)	119.9(2.0)	F(23)—C(23)—C(22)	121.9(2.6)
Hg(3)—C(11)—C(16)	119.8(2.0)	F(23)—C(23)—C(24)	118.0(2.7)
Hg(3)—C(11)—C(12)	118.0(2.6)	F(24)—C(24)—C(23)	115.8(2.7)
C(6)—C(1)—C(2)	116.1(2.6)	F(24)—C(24)—C(24)	123.9(2.9)
C(1)—C(2)—C(3)	120.2(2.5)	F(25)—C(25)—C(24)	120.4(2.9)
C(2)—C(3)—C(4)	121.2(2.8)	F(25)—C(25)—C(26)	119.1(2.8)
C(3)—C(4)—C(5)	119.6(3.1)	F(26)—C(26)—C(25)	119.8(2.6)
C(4)—C(5)—C(6)	119.5(3.1)	F(26)—C(26)—C(21)	117.5(2.7)
C(5)—C(6)—C(1)	123.4(2.9)	C(41)—C(31)—C(32)	119.9(2.7)
F(3)—C(3)—C(2)	118.1(2.6)	C(41)—C(31)—C(36)	120.5(2.7)
F(3)—C(3)—C(4)	120.7(2.7)	C(31)—C(41)—C(42)	116.3(2.7)
F(4)—C(4)—C(3)	118.6(2.8)	C(31)—C(41)—C(46)	121.4(2.8)
F(4)—C(4)—C(5)	121.7(3.0)	C(36)—C(31)—C(32)	119.6(2.8)
F(5)—C(5)—C(4)	120.9(3.0)	C(31)—C(32)—C(33)	121.2(3.0)
F(5)—C(5)—C(6)	119.6(2.9)	C(32)—C(33)—N(34)	124.8(3.2)
F(6)—C(6)—C(5)	115.4(2.7)	C(33)—N(34)—C(35)	117.7(3.0)
F(6)—C(6)—C(1)	121.2(2.7)	N(34)—C(35)—C(36)	124.8(3.2)
C(16)—C(11)—C(12)	118.0(2.6)	C(35)—C(36)—C(31)	116.0(2.8)
C(11)—C(12)—C(13)	119.3(2.7)	C(46)—C(41)—C(42)	122.2(3.0)
C(12)—C(13)—C(14)	122.7(2.9)	C(41)—C(42)—C(43)	120.8(3.2)
C(13)—C(14)—C(15)	116.1(2.9)	C(42)—C(43)—C(44)	115.7(3.2)
C(14)—C(15)—C(16)	120.2(2.8)	C(43)—C(44)—C(45)	118.0(3.5)
C(15)—C(16)—C(11)	123.0(2.7)	C(44)—C(45)—C(46)	126.4(3.6)
F(13)—C(13)—C(12)	123.2(2.7)	C(45)—C(46)—C(41)	116.7(3.0)
F(13)—C(13)—C(14)	114.0(2.7)		

plexes appear to be ruled out by the absence of change in other "ligand" bands at 653 cm^{-1} (DMF, DEF [10]) or 703 cm^{-1} (pyridine [11]). The far infra-red evidence also contra-indicates this form of bonding [11]. Charge transfer complexes between ligand and electronegatively-substituted C_6F_4 moiety appeared to be ruled out both by the lack of colour of the adducts and the lack of any solution UV bands additional to those of the separate components. Also absent were any major shifts in the C—D stretching frequency when deuteropyridine was used as the organic molecule; this appears to rule out strong hydrogen—fluorine interactions. X-ray powder patterns of the parent mercurial and of its 1 : 1 and 1 : 2 DMF adducts were all different, which would rule out clathrate formation; it is also difficult to visualise a clathrate system that will accept (a) molecules as diverse in size as acetone and triphenyl-phosphine, and (b) three discrete stoicheiometries.

The spectral data is thus consistent only with a relatively weak interaction between the "ligands" and the mercurial, probably of a Van der Waal's type.

TABLE 9

SHORT CONTACT DISTANCES (Å). ESTIMATED STANDARD DEVIATIONS ARE 0.04 Å EXCEPT WHERE QUOTED

(a) Distances less than 3.6 Å involving mercury atoms			
Hg(1)—Hg(2)	3.593(2) [a]	Hg(1)—F(13)	3.18 [a]
Hg(2)—Hg(3)	3.578(2) [a]	Hg(1)—F(23)	3.20 [a]
Hg(3)—Hg(1)	3.586(2) [a]	Hg(2)—F(6)	3.18 [a]
Hg(2)—F(26)	3.19 [a]	Hg(3)—F(3)	3.14 [a]
Hg(3)—F(16)	3.15 [a]	Hg(1)—F(26)	3.37
Hg(1)—C(33)	3.51	Hg(1)—N(34)	3.51
Hg(2)—F(23)	3.34	Hg(3)—C(44)	3.48
Hg(3)—F(3)	3.43		
(b) Intermolecular distances less than 3.4 Å involving light atoms			
C(1)—F(24)	3.31	C(6)—F(24)	3.21
C(4)—F(16)	3.33	F(4)—F(5)	3.03
C(5)—F(16)	3.17	F(5)—F(16)	3.39
C(11)—F(4)	3.27	C(13)—F(25)	3.17
C(15)—C(15)	3.35	C(16)—F(15)	3.36
F(13)—F(25)	3.04	F(14)—F(16)	3.22
F(16)—F(24)	3.19	F(16)—F(25)	3.07
C(24)—F(6)	3.11	C(25)—F(6)	3.37
C(25)—F(13)	3.30	F(23)—F(26)	3.20
F(25)—F(15)	2.92	C(31)—F(23)	3.37
C(32)—F(6)	3.30	C(33)—F(6)	3.23
C(36)—F(13)	3.26	C(42)—F(24)	3.21
C(43)—F(3)	3.26	C(44)—F(3)	3.40
C(44)—F(15)	3.35	C(46)—F(26)	3.40

[a] Intramolecular values, all others are intermolecular.

The thermal decomposition data would normally have been interpreted in terms of the making or breaking of chemical bonds as the rate-controlling step, as in the cobalt complexes of known structure [12,13] which gave similar TG results (Tables 2, 3). Unfortunately, attempts to obtain comparable data from mercury complexes of known structure were unsuccessful: bis(pentafluorophenyl)mercury [14], mercury(II) chloride [15] and mercury(II) bromide [11] were all too volatile for such a study, whereas the 1 : 2 mercury(II) iodide-pyridine complex [10] gave ambiguous isothermal results. The cobalt complexes gave activation energies somewhat higher than those obtained for the mercurial adducts and it can be noted that the adducts, whilst less stable thermally than the cobalt complexes (no adduct resisted decomposition much above the boiling-point of the free solvent) are apparently more stable than the mercury(II)-pyridine complexes, which effloresce to the unsolvated state at room temperature.

The crystal structure of the 1 : 1 adduct of perfluorotribenzo[*b*,*e*,*h*][1,4,7]-trimercuronin and 4-phenyl pyridine shows that it is probably bound together by Van der Waal's forces between the permanent dipole of the organic molecule and induced dipoles in the mercurial. The relative spatial arrangement of the two molecules rules out charge-transfer effects and hydrogen—fluorine bonding. Furthermore electron-donation from the nitrogen to any of the mercury atoms is disproved by the closest Hg—N contact of 3.51 Å which compares with 2.60 Å in the 1 : 2 complex between mercury(II)chloride and pyridine [15] and 2.18 Å in the 1 : 1 complex between mercury(II)chloride and 2,4,6-trimethylpyridine [16]. The nitrogen was located at position (34) rather than (44) as this gave physically reasonable temperature factors for both atoms.

In addition to the direct dipolar interaction, the effect of the 4-phenylpyridine is to increase the separation between mercurial molecules, and thus diminish the repulsion between the negatively charged fluorine atoms which surround the edge of the planar mercurial. The dipole is apparently important because simple hydrocarbons such as benzene and toluene do not form adducts. Decomposition of all the adducts in solution, revealed by UV, IR and ^{19}F NMR spectroscopy, is consistent with the type of interaction postulated, although complexes of bis(pentafluorophenyl)mercury also decompose in solution [17].

The bond lengths and angles are within normal values: the carbon—mercury bonds can be compared with 2.09 and 2.10 Å in bis(pentafluorophenyl)mercury [18] and 2.10 Å in bis(2,3,4,5-tetrafluorophenyl)mercury [4]. The carbon—mercury—carbon bond angles are all close to the ideal 180°. One consequence of adduct formation appears to be an increase in intermolecular mercury—mercury separations: the closest contacts in this structure are 5.15 Å [Hg(3)—Hg(3)] and 5.71 Å [Hg(1)—Hg(2)] compared with 3.44 Å in the orthorhombic and 3.67 Å in the monoclinic forms of the analogous tribenzo[*b*,*e*,*h*]-[1,4,7]trimercuronin. The intra-molecular Hg—Hg separations of 3.593, 3.586 and 3.578 Å reveal more about the approximation to ideal D_{3h} symmetry in the mercurial than anything else, since the *o*-phenylene bridges hold the metal atoms in a rigid matrix.

The structure also proves that perfluoro-*o*-phenylene mercury is a trimer as initially proposed by Sartori [3] and consistent with *o*-phenylenemercury itself [1,2].

Acknowledgements

We thank Dr. A.G. Briggs for the Raman Spectra, Dr. R.E. Humphries for the far IR spectra, and gratefully thank the S.R.C. for a grant to D.A.W.

References

1 D.S. Brown, A.G. Massey and D.A. Wickens, Acta Cryst. B, 34 (1978) 1695.
2 D.S. Brown, A.G. Massey and D.A. Wickens, Inorganica Chimica Acta, 44 (1980) L193.
3 P. Sartori and A. Golloch, Chem. Ber., 101 (1968) 2004.
4 D.S. Brown, A.G. Massey and D.A. Wickens, J. Organometal. Chem., 194 (1980) 131.
5 J.H. Sharp, G.W. Brindley and B.N.N. Achar, J. Amer. Ceram. Soc., 49 (1966) 379.
6 V. Satava and F. Skvara, J. Amer. Ceram. Soc., 52 (1969) 591.
7 G. Sheldrick; SHELX, a Program for Crystal Structure Determination, 1976.
8 P. Main, L. Lessinger, M.M. Woolfson, G. Germain and J.P. Declercq, MULTAN 74, a System of Computer Programs for the Automatic Solution of Crystal Structures from X-ray Diffraction Data, 1974.
9 C.K. Johnson, ORTEP, ORNL-5138, U.S. Department of Commerce, Springfield, Va., 22161.
10 M.A.J. Jungbauer and C. Curran, Nature, 202 (1964) 290.
11 R.M. Barr, M. Goldstein and W.D. Unsworth, J. Cryst. Mol. Structure, 4 (1974) 165.
12 P.J. Clarke and H.J. Milledge, Acta Cryst. B, 31, (1975) 1543 and 1554.
13 J.D. Dunitz, Acta Cryst., 10 (1957) 307.
14 A.J. Canty and B.M. Gatehouse, J. Chem. Soc. Dalton, (1972) 511.
15 D. Grdenić and I. Krstanović, Arhiv. Kemi, 27 (1955) 143.
16 S. Kulpe, Z. Anorg. Allg. Chem., 349 (1967) 314.
17 A.J. Canty and G.B. Deacon, Austr. J. Chem., 24 (1971) 489.
18 N.R. Kunchur and N. Mathew, Chem. Commun., (1966) 71.